Icing of Wind Turbine Blades Obtained by an Inverse Design Process

Laszlo E. Kollar
Savaria Institute of Technology
ELTE Eötvös Loránd University, Budapest, Hungary
e-mail: kl@inf.elte.hu

Rakesh Mishra
School of Computing & Engineering
University of Huddersfield, Huddersfield, UK
e-mail: r.mishra@hud.ac.uk

ABSTRACT

An inverse design process is applied to determine the shape of the two dimensional section of wind turbine blades, and the effects of ice accretion on the aerodynamics of the blade is evaluated. The bare blade shape is obtained from a prescribed pressure or velocity distribution around a two dimensional section of the blade, using the Garabedian-McFadden technique. Then, the icing of this blade section is simulated under defined ambient conditions in order to predict change in the shape of the blade due to ice accretion. The aerodynamic performance of the wind turbine is validated by calculating the lift coefficient and the drag coefficient of the ice-covered blade and by comparing these values to those obtained on the bare blade. The procedure presented will contribute towards the design of blade shapes that can enable wind turbines to operate under a wide range of ambient conditions.

KEYWORDS

Aerodynamics, Droplet motion, Icing, Inverse design, Simulation, Wind turbine

INTRODUCTION

Ice accretion on rotor blades in cold climates considerably worsens the aerodynamic performance of wind turbine systems. Typically, ice accretion results in reduction of lift generation and increase in drag leading to power loss which may go up to 30% at sites with particularly high risk of icing. Furthermore, ice accumulation also affects safety and lifetime of the wind turbine systems [1, 2]. Considerable research efforts have been directed in order to study the effects of icing on wind turbine blades. Bose [3] observed ice formation on horizontal axis wind turbine blades, and reported icing profiles that were formed in natural glaze icing events. Both experimental and numerical research has been performed in order to study the effects of icing on wind turbine performance, and the reduction in annual energy production was obtained to be above 20% in extreme cases [4, 5].

The aerodynamics of the rotor blades of wind turbines affects substantially the performance of the wind turbine. The main challenge in the design of rotor blades is to find the relationship between its shape and its aerodynamic properties. The designer targets given performance criteria, which is then tested either experimentally or computationally. Then, the geometry is modified based on the results obtained, and the design loop is repeated until an adequate blade design is found. Inverse design methods generate geometry automatically for a pre-defined aerodynamic performance. Design processes developed up to now do not consider ice

accretion on the blade, which changes the geometry, and thereby, it modifies the aerodynamic properties. Nevertheless, careful study of the prevailing icing conditions of the wind farm under investigation as well as the effects of icing under those conditions on the aerodynamics of the blade may help improve the process of choosing a blade shape so that the aerodynamic degradation due to ice accretion is minimized.

Garabedian & McFadden [6] developed an iterative procedure to design swept wings. This scheme was later modified in [7], which allowed design for a wide range of geometry with prescribed surface pressures. The authors referred to this technique as the modified Garabedian-McFadden method. The present paper applies an inverse design methodology in two dimension (2D), which is based on the modified Garabedian-McFadden method. First, this process provides the shape of the 2D section of the bare blade. Then, the air velocity field in the proximity of this blade is determined; where the motion of water droplets is simulated. The local ratio of droplets that hit the blade surface is predicted after considering the collision of droplets to the blade surface. The local ratio of droplets that freeze to the blade surface is calculated from the heat balance, which helps predict the mass and shape of ice accretion at different locations around the blade. These computational steps of are implemented in Matlab assuming potential flow. Finally, the flow around the iced blade is simulated, the lift and drag coefficients are calculated and compared to those obtained for a bare blade. Since the flow around the iced blade is highly viscous, potential flow approach cannot be applied. Therefore, the ANSYS Fluent computational fluid dynamics software was used for the simulation of flow around the iced blade and for the calculation of aerodynamic coefficients. The above methodology was repeated assuming different performance criteria, consequently, different bare blade shapes, as well as different icing conditions. The results obtained provide information for the designer to find the blade shape so that ice accretion influences aerodynamic performance for the least possible extent.

The subsequent sections first describe the methodology, then its application is discussed for two icing conditions, in-cloud icing and freezing drizzle, and it is applied for three blade shapes corresponding to three different performance criteria.

METHODOLOGY

This section describes the methodology including the following steps: (i) inverse design process to obtain the shape of the 2D section of the bare blade; (ii) calculation of the air velocity field; (iii) finding the mass and shape of ice accretion; and (iv) simulation of air flow around the iced blade and calculation of aerodynamic coefficients.

Inverse design process for bare blades

The blade shape is determined according to a prescribed velocity (or pressure) distribution using the modified Garabedian-McFadden technique [7]. An initial blade shape is chosen, and the deviation of velocity distribution near the surface from the target velocity distribution is expressed by the surface ordinate y, the slope of the surface $\mathrm{d}y/\mathrm{d}x$, and the second derivative of the surface, $\mathrm{d}^2y/\mathrm{d}x^2$. The change in the surface ordinate is denoted by Δy. Its positive value means that the profile moves upward on the upper surface and downward on the lower surface. The equation to be solved for the change in the position of the blade surface is the following

$$A\Delta y + B\frac{\mathrm{d}(\Delta y)}{\mathrm{d}x} - C\frac{\mathrm{d}^2(\Delta y)}{\mathrm{d}x^2} = V_{tar}^2 - V_{pr}^2 \qquad (1)$$

where V_{pr} and V_{tar} are the present and target velocities, respectively, and A, B and C are constants that should be large enough to avoid the shape from changing too much in one step. The following values were applied in the present study: A = 1000; B = 100; C = 400. These values were chosen to satisfy the condition that the number of iterations should be the smallest when the free stream velocity is in the range of interest (i.e. up to 30 m/s). In the calculation, both of the top and bottom blade surfaces are divided into n subdomains. The change of ordinate at the leading edge Δy_1 and at the trailing edge Δy_n is zero. The derivatives of Δy_i, $i = 2,\ldots,n-1$ in each subdomain are written in discrete form, and the $n-2$ equations are organized in matrix form. The matrix obtained is tridiagonal; thus, the matrix equation can be solved by the tridiagonal matrix algorithm or Thomas algorithm [8, 9].

Air velocity field around bare blade

The air velocity field in the computational domain around the turbine blade is determined using a panel method [10]. The panel method is applicable for 2D, incompressible flow around single-element aerofoils where the Laplace's equation is solved for the stream function. The governing equation is the Laplace's equation for the stream function ψ, and it is written in the following form

$$\frac{\partial^2 \psi}{\partial x^2} + \frac{\partial^2 \psi}{\partial y^2} = 0 \qquad (2)$$

This equation is recast into an integral equation. The surface is divided into panels, and the integral is approximated by an algebraic expression on each of these panels. Velocities are obtained as solutions of a system of linear algebraic equations [10].

Mass and shape of ice accretion

Ice accretion is caused by supercooled water droplets that impinge on and freeze at the blade surface. In order to simulate this process, first the droplet trajectories are determined, and local collision efficiencies are calculated along the blade surface. However, not all of the collided droplets freeze to the surface and contribute to the ice accretion. Therefore, the heat balance is applied on the blade surface, which provides the local accretion efficiency along the entire surface. The total mass of droplets in each subdomain on the surface is multiplied by the local accretion efficiency so that the relative mass and then the relative thickness of ice can be determined locally.

Rate of icing. The maximum flux density of water droplets that may contribute to the ice growth on a unit projection area F is the product of mass concentration w and the velocity v of particles relative to the icing object. The rate of icing, i.e. the accreted ice mass M in unit time t, is expressed in the form [11]

$$\frac{\mathrm{d}M}{\mathrm{d}t} = \alpha_1 \alpha_2 \alpha_3 w v F \qquad (3)$$

The maximum flux density is reduced by three correction factors that should be determined in order to obtain the rate of icing. These are (i) the collision efficiency α_1, i.e. the ratio of the flux density of the particles that hit the icing object to the maximum flux density; (ii) the sticking efficiency α_2, i.e. the ratio of the flux density of the particles that stick to the object to the flux density of the particles that hit the object; and (iii) the accretion efficiency α_3, i.e. the ratio of the rate of icing to the flux density of the particles that stick to the object [11]. The simulation of droplet trajectories around the blade provides information about the ratio of the particles that hit the blade surface, from which the collision efficiency is obtained. If snow

accretion is not considered, then the sticking efficiency may be assumed to be 1, because water droplets do not bounce. Finally, the accretion efficiency is obtained from the heat balance of droplets on the blade surface. Since these correction factors are calculated locally along the blade surface, the rates of icing at different positions along the turbine blade and the relative local ice thickness on the blade surface can be determined.

Collision efficiency. Droplet trajectories are obtained from the droplet equation as detailed in [12]. Integrations of this equation provide droplet velocity and droplet position in each time step. The local collision efficiency at the point of impact is determined from the ratio of the initial perpendicular separation of trajectories of two nearby droplets to the final separation of their respective impact points on the blade surface. Assume that two droplets leaving from neighbouring initial positions (x_0;$y_{0,j}$) and (x_0;$y_{0,j+1}$) hit the blade surface at positions (x_j,y_j) and (x_{j+1},y_{j+1}), then the local collision efficiency in the interval limited by the latter points is calculated as follows

$$\alpha_1 = \frac{\left| y_{0,j+1} - y_{0,j} \right|}{\sqrt{\left(x_{j+1} - x_j\right)^2 + \left(y_{j+1} - y_j\right)^2}} \tag{4}$$

The local collision efficiency depends on droplet size. Therefore, the droplet size distribution (DSD) is discretized by dividing the droplet size spectrum into bins, and a local collision efficiency is calculated for droplets in each bin. Then, they are multiplied by the mass-based relative frequency of that droplet size in the DSD, and the sum of these products provides the local collision efficiency.

Accretion efficiency. The local accretion efficiency α_3 is determined from the heat balance [11, 13]

$$Q_f + Q_v + Q_a = Q_c + Q_e + Q_l + Q_s \tag{5}$$

where Q_f is the latent heat released during freezing, Q_v is the kinetic heating of air, Q_a is the heat released in cooling the ice from its freezing temperature to the surface temperature, Q_c is the convective heat transfer, Q_e is the evaporative heat transfer, Q_l appears due to the temperature difference between the impinging droplets and the icing surface, and Q_s is heat loss due to long-wave radiation. The latent heat Q_f includes the accretion efficiency; thus, if all the other relevant parameters are substituted into the heat balance then the accretion efficiency can be determined.

Air flow around iced blade and aerodynamic coefficients

The effects of ice on the aerodynamics of the wind turbine blade are evaluated by comparing the lift and drag coefficients of the bare and iced blades. Ice on the blade decreases the lift coefficient and increases the drag coefficient; however, the extent of modification of aerodynamic parameters depends on the icing conditions and the blade shape that is determined by the performance criteria. This will be discussed in detail in the next section.

The shape of iced blade was obtained using the computation described earlier, which was implemented in Matlab. This blade shape served as input for further computation that was carried out using ANSYS Fluent computational fluid dynamics software. The computational domain was chosen so that it extended four times the chord length before the leading edge and three times the chord length after the trailing edge. The height of the computational domain extended twice the chord length above and below the $y = 0$ position that connects the leading edge and the trailing edge. Triangular mesh was applied where the minimum and maximum

face sizes were 0.2% and 5%, respectively, of the chord length. The flow was modelled by the k-ε model with standard wall functions. Velocity at the inlet of the computational domain was prescribed according to the free stream velocity as boundary condition. Settings of spatial discretization included Green-Gauss node-based gradient evaluation, standard scheme for the pressure equation, and second order upwind scheme for the momentum and energy equations. Solution was initialized from the inlet, and calculation ran for 500 iterations. Results obtained after the calculation included aerodynamic forces and coefficients.

APPLICATION

The methodology described in the previous section is applied for different ambient conditions and different target velocity distributions. The chosen ambient conditions correspond to two substantially different icing events: in-cloud icing and freezing drizzle. The target velocity distributions are chosen so that they can be produced around blades with significantly different shapes, and the lift coefficients of these blades also differ from each other.

Although meteorological conditions vary to some extent everywhere, typical icing conditions may be observed in the geographical location where the wind turbine under examination is situated. Different icing conditions contribute to different degree to the reduction in lift and to the increase in drag. However, the degree of this aerodynamic degradation also depends on the shape of the turbine blade. If appropriate blade shape is chosen, considering the prevailing icing conditions of the geographical location, then the rate of reduction in lift and the rate of increase in drag can be minimized. In the design process, the blade shape is chosen from the velocity (or pressure) distribution that is prescribed according to performance criteria. Consequently, if the prevailing icing conditions occur frequently in the location of the wind turbine, it may be favourable to modify the velocity distribution so that icing on the resulting blade shape leads to less severe aerodynamic degradation. The discussion in this section will reveal how two different icing conditions modify the aerodynamic performance of wind turbines with three different blade shapes.

Icing conditions and blade shapes

The two icing conditions taken into account correspond to in-cloud icing and freezing drizzle events. These conditions are considered by some typical values of the thermodynamic parameters as shown in Table 1. The angle of attack was set at 0 deg in both cases.

TABLE 1. Thermodynamic parameters describing the icing conditions considered

Icing condition	Wind speed	Air temperature	Liquid water content	Median volume diameter
	(m/s)	(°C)	(g/m^3)	(μm)
In-cloud icing	20	–10	0.3	27
Freezing drizzle	10	–5	1.5	62

In inverse design processes the blade shape is not known, but they are determined from target velocity distributions prescribed according to performance criteria. In the present study, target velocity distributions were applied which may be measured around NACA2412, NACA4412 and NACA6409 aerofoils. These are shown pictorially in Fig. 1. The shape of NACA2412 is thicker, its form is closer to a symmetric shape. The shape of NACA4412 is more asymmetric, and the shape of NACA6409 is the thinnest and most asymmetric. In this order, the blades cause higher and higher flow turning at the trailing edge, and consequently, the lift

is greater and greater. The computation in the inverse design process was initiated from a symmetrical blade shape, the NACA0012 aerofoil. The inverse design process found the blade shapes in all the three cases quickly, i.e. after 10-50 iterations when both of the top and bottom blade surfaces were divided into 50 subdomains, and the average error in the position of these subdomains was set at 10^{-4} times the thickness of the aerofoil. The airflow field around these aerofoils for free stream velocity of 10 m/s were obtained as shown in Fig. 1.

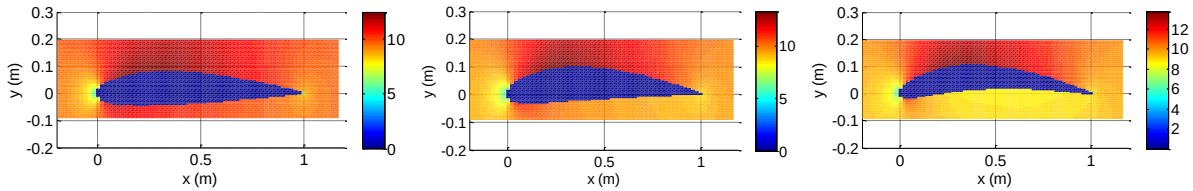

Figure 1. Airflow fields around aerofoils, a) NACA2412, b) NACA4412, c) NACA6409

Aerodynamic coefficients of bare and iced blades

The shapes of ice accretion on the blade under the two icing conditions are significantly different due to the dissimilar ambient conditions. The effects of thermodynamic parameters listed in Table 1 on the mass and shape of ice accretion have been studied extensively, see e.g. [14]. Iced shapes of the NACA4412 blade under the two icing conditions are drawn in Fig. 2.

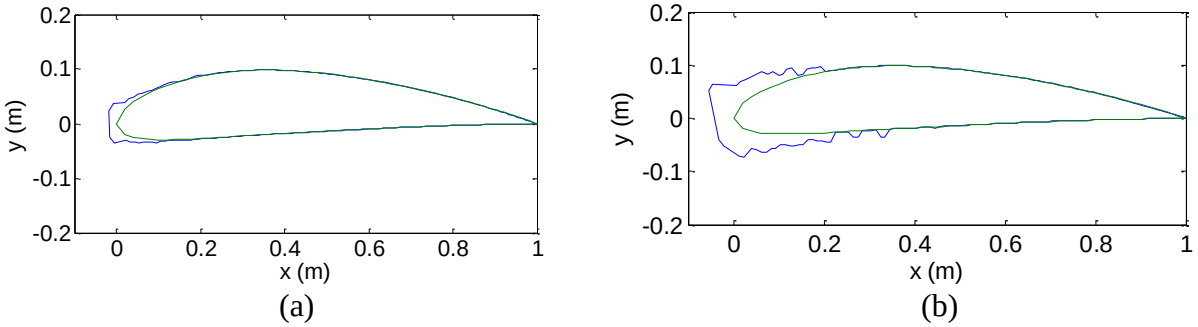

Figure 2. Iced shapes of the NACA4412 blade, a) in-cloud icing, b) freezing drizzle

The blade shape, and consequently, the aerodynamic coefficients, change more significantly under freezing drizzle conditions than under in-cloud icing conditions. The lift coefficient C_L decreases, whereas the drag coefficient C_D increases. These changes will be evaluated altogether by the variation of one parameter: the ratio of lift and drag coefficients C_L/C_D. Tables 2 and 3 list the values of these aerodynamic parameters for different blade shapes under the conditions of in-cloud icing and freezing drizzle, respectively. Note that the values are slightly different under the two conditions even for the bare blade, because the free stream velocities are different. Tables 2 and 3 also reveal in their last column to what extent the ratio of lift and drag coefficients reduces due to ice accretion. As expected, this reduction is significantly greater under freezing drizzle conditions than under in-cloud icing conditions. More precisely, this ratio reduces to its 10 to 30% under freezing drizzle conditions; whereas the ratio C_L/C_D for the iced blade is almost half of that for the bare blade under in-cloud icing conditions. In both cases, the reduction is the smallest, or in other words, the value in the last column is the greatest for the NACA4412 aerofoil. According to the results obtained, the blade that ice accretion has the less severe impact on from the point of view of aerodynamics is the NACA4412.

TABLE 2. Aerodynamic coefficients under in-cloud icing conditions

Aerofoil	C_L	C_D	C_L/C_D	$\frac{(C_L/C_D)_{\text{iced}}}{(C_L/C_D)_{\text{bare}}}$
NACA2412, bare	0.237	0.012	19.75	
NACA2412, iced	0.212	0.024	8.83	0.45
NACA4412, bare	0.509	0.013	39.15	
NACA4412, iced	0.449	0.024	18.71	0.48
NACA6409, bare	0.708	0.012	59.00	
NACA6409, iced	0.656	0.024	27.33	0.46

TABLE 3. Aerodynamic coefficients under freezing drizzle conditions

Aerofoil	C_L	C_D	C_L/C_D	$\frac{(C_L/C_D)_{\text{iced}}}{(C_L/C_D)_{\text{bare}}}$
NACA2412, bare	0.239	0.013	18.38	
NACA2412, iced	0.158	0.082	1.93	0.10
NACA4412, bare	0.466	0.014	33.29	
NACA4412, iced	0.387	0.043	9.00	0.27
NACA6409, bare	0.710	0.013	54.62	
NACA6409, iced	0.574	0.047	12.21	0.22

CONCLUSION

An inverse design process has been applied to determine shape of the 2D section of wind turbine blades, and the effects of icing on the aerodynamics of the blade obtained have been evaluated by comparing the change in the lift and drag coefficients due to ice accretion. The study considers three different blade shapes and two different icing conditions. Results reveal that ice accretion has the less severe effect on the aerodynamics of the blade with the shape of NACA4412 aerofoil among the three aerofoils examined. This conclusion suggests that the aerodynamics of thick shapes that are closely symmetric as well as the aerodynamics of greatly asymmetric shapes worsens more significantly due to ice accretion than the aerodynamics of a blade with shape in between. In order to confirm this finding and incorporate it in the design process, further study is recommended including simulations with additional shapes and a proposition for the modification of the target velocity distribution when it is preferable for reducing ice accretion.

NOMENCLATURE

A, B, C	constants of the Garabedian-McFadden method
C_D, C_L	drag and lift coefficients
F	projection area on the icing surface
M	accreted ice mass
n	number of subdomains on the top and bottom of blade surface
Q	heat
t	time
v	velocity of particles reaching the icing object
V_{pr}, V_{tar}	present and target velocities in the Garabedian-McFadden method

w	mass concentration of particles reaching the icing object
x, y	coordinates in the horizontal and vertical directions
$\alpha_1, \alpha_2, \alpha_3$	collision efficiency, sticking efficiency, accretion efficiency
ψ	stream function

ACKNOWLEDGMENT

This paper was supported by the János Bolyai Research Scholarship of the Hungarian Academy of Sciences. The financial support of EFOP-3.6.1-16 project: "Innovative processing technologies, applications of energy engineering and implementation of wide range techniques for microstructure investigation" within a Széchenyi 2020 program is gratefully acknowledged.

REFERENCES

1. Seifert, H., and Richert, F., Aerodynamics of Iced airfoils and their Influence on Loads and Power Production, *European Wind Energy Conference*, Dublin, Ireland, pp. 458-463, 1997.
2. Hau, E., *Wind Turbines: Fundamentals, Technologies, Application*, Economics, Springer-Verlag, Berlin, Germany, 2006.
3. Bose, N., Icing on a small horizontal-axis wind turbine - Part 1: Glaze ice profiles, *Journal of Wind Engineering and Industrial Aerodynamics*, Vol. 45, pp. 75-85, 1992.
4. Barber, S., Wang, Y., Chokani, N., Abhari, R. S., The Effect of Ice Shapes on Wind Turbine Performance, *13th International Workshop on Atmospheric Icing of Structures*, Andermatt, Switzerland, 2009.
5. Yirtici, O., Tuncer, I. H., Ozgen, S., Ice Accretion Prediction on Wind Turbines and Consequent Power Losses, *Journal of Physics: Conference Series* 753, 2016.
6. Garabedian, P., McFadden, D., Design of Supercritical Swept Wings, *AIAA Journal*, Vol. 20, pp. 289-291, 1982.
7. Malone, J. B., Vadyak, J., Sankar, L. N., Inverse Aerodynamic Design Method for Aircraft Components, *J. Aircraft*, Vol. 24, pp. 8-9, 1987.
8. Conte, S. D., de Boor, C., *Elementary Numerical Analysis*, McGraw-Hill, Singapore, 1981.
9. Kollar, L. E., Mishra, R., Jain, A., Inverse Design of Blade Shapes for Vertical Axis Wind Turbines, *6th International and 43rd National Conference on Fluid Mechanics and Fluid Power*, Allahabad, India, 2016.
10. http://soliton.ae.gatech.edu/people/lsankar/AE3903/
11. Makkonen, L., Models for the growth of rime, glaze, icicles and wet snow on structures, *Phil. Trans. R. Soc. Lond.* A, Vol. 358, pp. 2913-2939, 2000.
12. Kollár, L. E., Farzaneh, M., Modeling the evolution of droplet size distribution in two-phase flows, *Int. J. of Multiphase Flow*, Vol. 33, pp. 1255-1270, 2007.
13. Makkonen, L., Laakso, T., Marjaniemi, M., Finstad, K. J., Modelling and prevention of ice accretion on wind turbines, *Wind Engineering*, Vol. 25, No. 1, pp. 3-21, 2001.
14. Lozowski, E. P., Stallabras, J. R., Hearty, P. F., The Icing of an Unheated, Nonrotating Cylinder. Part I: A Simulation Model, *Journal of Climate and Applied Meteorology*, Vol. 22, pp. 2053-2062, 1983.